# Investigation of hard magnetic properties of nanocomposite Fe-Pt magnets by micromagnetic simulation

Chuan-bing Rong, Hong-wei Zhang, Xiao-bo Du, Jian Zhang,
Shao-ying Zhang, and Bao-gen Shen
*State Key Laboratory of Magnetism, Institute of Physics and Centre for Condensed Matter Physics, Chinese Academy of Sciences, Beijing 100080, China*

(Received 13 February 2004; accepted 22 July 2004)

Micromagnetic finite element method is used to simulate magnetic properties of $FePt/Fe_3Pt$ exchange-coupled nanocomposites. Numerical results show that the maximum energy product $(BH)_{max}$ about 34.6 MGOe can be obtained for the 3-nm-scale isotropic magnets with the volume fraction of soft $Fe_3Pt$ phase $v_s=15\%$. The appearance of touched soft grains causes the decrease of reduced remanence $m_r$ when $v_s$ exceeds 20%. Coercivity decreases with the simultaneous decrease of $D_s$ and $D_h$, where $D_s$ and $D_h$ are the grain sizes of soft and hard phases, respectively. Only under the prerequisite of sufficiently large $D_h$, the coercivity can be improved remarkably by decreasing $D_s$ below twice the domain wall width of hard phase. © *2004 American Institute of Physics*.
[DOI: 10.1063/1.1792812]

## I. INTRODUCTION

Nanocomposite magnets consisting of exchange-coupled hard and soft magnetic phases have attracted much attention due to their giant energy products $(BH)_{max}$.[1–8] A critical requirement for the exchange coupling is that the dimension of the soft phase should be comparable to twice the domain wall width of the hard phase, which is typically on the order of 10 nm according to the quasi-one-dimensional model.[1] Additionally, the alignment of the easy axes of hard phase is needed for high performance. However, the ideal nanostructured composites are very difficult to prepare experimentally by using conventional techniques like rapid solidification or mechanical alloying.[3–6] The permanent magnets prepared in this way are isotropic and their soft grain sizes are larger than 10 nm. As a consequence, their $(BH)_{max}$ are only about 20 MGOe. Using magnetron sputtering techniques,[7] Liu *et al.* obtained a $(BH)_{max}$ up to 50 MGOe in Fe-Pt nanocomposites with the texture of hard grains.[8] Recently, grain sizes of isotropic nanocomposite $FePt/Fe_3Pt$ have been decreased to 5 nm by nanoparticle self-assembly method,[9–12] where FePt is a magnetically hard phase and $Fe_3Pt$ a soft phase. Thus, it is interesting to investigate how large $(BH)_{max}$ can be achieved for isotropic magnets in future experiments.

Isotropic nanocomposite permanent magnets are of a special benefit to commercial application. How large is the theoretical limit of $(BH)_{max}$ and what kind of behavior may be observed when the grain size is smaller than 10 nm? In this work, we try to answer such questions and make clear the grain size dependencies of remanence and coercivity for the nanocomposites with small grains.

## II. SIMULATION MODEL

Micromagnetics based numerical simulation is an effective tool to investigate magnetization process.[13–15] There are different numerical schemes in micromagnetics. For example, the Landau-Gilbert equation is usually used for dynamic calculation. The static calculation minimizing the energy of the system is widely used to find a magnetization distribution, so it is approved for the simulation of a magnetic hysteresis loop. By means of finite element method, the total magnetic Gibbs free energy $G$,

$$G = \Phi_K + \Phi_{ex} + \Phi_S + \Phi_H, \tag{1}$$

is minimized with respect to the direction of the spontaneous polarization $\mathbf{J}_s$. Here, $\Phi_K$ is the magnetocrystalline anisotropy energy, $\Phi_{ex}$ is the exchange energy, $\Phi_S$ is the strayfield energy, and $\Phi_H$ is the Zeeman energy in an external field $\mathbf{H}_{ext}$. In order to use standard numerical optimization methods, it is necessary to find a discrete form of the energy function as a function of $\mathbf{J}_s$ only. All energy terms but the strayfield energy depend only on the local magnetization. The long-range nature of the dipolar interaction can be mathematically eliminated by introducing a vector potential $\mathbf{A}$ as shown by Brown.[16] Thus, the strayfield energy $\Phi_S$ can be approximated by an upper bound as follows:

$$\Phi_S \leqslant \frac{1}{2\mu_0}\int (\nabla \times \mathbf{A} - \mathbf{J}_s)^2 d^3r. \tag{2}$$

The resulting open-boundary problem can be treated by a parallelepipedic shell transformation, which transforms the infinite exterior space of the magnet on a shell around the magnet.[17] The finite element discretization of Eq. (1) leads to a large-scale nonlinear optimization problem. The so-called preconditioned, limited memory quasi-Newton conjugate gradient method[18] is proved to be the most efficient for such large-scale problems. We must point out that the present micromagnetic algorithm does not take into account thermally activated processes. The magnetic parameters used for the calculation at room temperature are as follow: [19–21] $J_s^{FePt}=1.38$ T, $K_1^{FePt}=6.6\times10^6$ J/m$^3$, $A^{FePt}=1.0\times10^{-11}$ J/m, and $J_s^{Fe_3Pt}=2.0$ T. It is reasonable to assume that $K_1^{Fe_3Pt}=K_1^{FePt}/100$ and $A^{Fe_3Pt}=2A^{FePt}$ since $Fe_3Pt$ is the magnetic

 

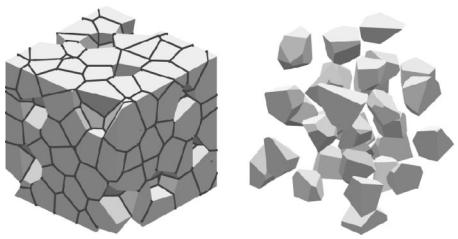

FIG. 1. The microstructure of FePt/$Fe_3Pt$ magnet consisting of 216 irregular shaped grains. The left is the distribution of FePt grains and the right is that of $Fe_3Pt$ grains. The volume fraction of $Fe_3Pt$ $v_s$ is 15%.

soft phase. Thus, the domain wall width $\delta_B = \pi\sqrt{A/K_1}$ of FePt is about 3.9 nm.

Our recent calculations,[22] and those of Griffiths *et al.*,[23] show that the unsuitable sizes of computational region and finite element can lead to large numerical errors. To avoid systematic error, we have calculated the demagnetization curves of the single phase FePt magnets using the samples with 216 and 729 grains. Although the demagnetization curves of the sample with 729 grains are smoother than those of the sample with 216 grains, the relative difference of the extracted coercivity (remanence) between two samples is smaller than 3%. Thus, the sample consisting of 216 irregularly shaped grains is adopted for saving computing time. The finite element mesh generator (GEOMPACK package),[24] which can decrease element size near corners and grain boundaries, guarantees an accurate numerical treatment while keeping the number of element small. Since the main task of this work is to investigate the magnetization reversal of the nanocomposites with small grains, the number of finite elements (about 70 000) can be kept unchanged for saving the long computing time. Thus, the element size near grain boundaries is about 0.5 nm and that of the grain center is about 1 nm for the sample with mean grain diameter $D = 5$ nm. According to our recent micromagnetic calculations,[22] the numerical error is less than 8% even for the sample with $D = 30$ nm.

Figure 1 shows the microstructure of FePt/$Fe_3Pt$ two-phase magnet containing 15%$Fe_3Pt$ as an example. The distribution of the easy axes for hard grains is chosen randomly to simulate the isotropic magnet. The transmission electron microscopy investigations of the FePt/$Fe_3Pt$ nanocomposite magnet obtained by nanoparticle self-assembly method [11] show that the $Fe_3Pt$ phase is uniformly dispersed into the FePt matrix. This microstructure is different from that of the bulk nanocomposite magnets produced by conventional methods in which soft phases are randomly assigned to each grain. To simulate the special microstructure, soft grains are homogeneously distributed in the hard phase matrix and do not touch each other in our simulated models.

## III. RESULTS AND DISCUSSION

Keeping the volume fraction of soft $Fe_3Pt$ phase $v_s = 15\%$ and $D_h = D_s = D$, the magnetization reversal behaviors are simulated for $D$ varying from 3 nm to 30 nm, where $D_h$ and $D_s$ are the mean sizes of hard and soft grains, respectively. Figure 2 shows the typical demagnetization curves for $D = 3, 4, 8, 9$, and 30 nm. The demagnetization curves are

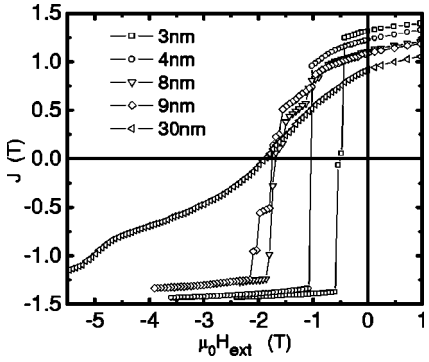


FIG. 2. Typical demagnetization curves of the samples with $D = 3$, 4, 8, 9, and 30 nm and $v_s = 15\%$.

calculated starting from the completely saturated state. A good single-phase magnetic behavior is observed for $D < 8$ nm.

The influences of $D$ on reduced remanence $m_r$ [$=J_r/J_s$, where $J_r$ is the remanence and $J_s$ is equal to $v_s J_s^{Fe_3Pt} + (1 - v_s) J_s^{FePt}$], coercivity $H_c$, and $(BH)_{max}$ are shown in Fig. 3. It is found that the value of $m_r$ is far larger than 1/2. According to the Stoner-Wohlfarth theory,[25] $m_r$ is 1/2 for an assembly of isotropic small noninteracting particles with uniaxial anisotropy. However, intergrain exchange coupling plays an important role in nanoscaled permanent magnets.[13–15,26,27] The competition between magnetocrystalline anisotropy and exchange interaction causes a smooth transition of magnetization from one easy direction to the other over a width of $\delta_B$. Then the extension of the exchange coupling can be described as the ratio of the coupled volume to a grain volume.

$$v_{ex} = [(D/2)^3 - (D/2 - \delta_B)^3]/(D/2)^3. \quad (3)$$

Only the magnetization in the exchange coupling region can contribute to the remanence enhancement. The decrease of $D$ results in the increase of $v_{ex}$ as given in Eq. (3). Thus, $m_r$ increases with the decline of $D$. The dependence of $m_r$ on $D$

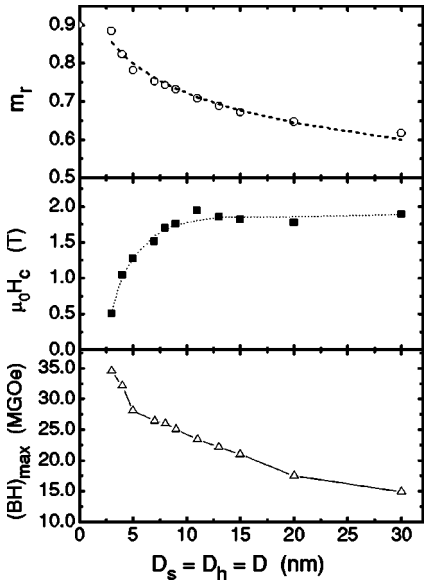


FIG. 3. $m_r$, $H_c$, and $(BH)_{max}$ as functions of $D$ for the magnets with $v_s = 15\%$.

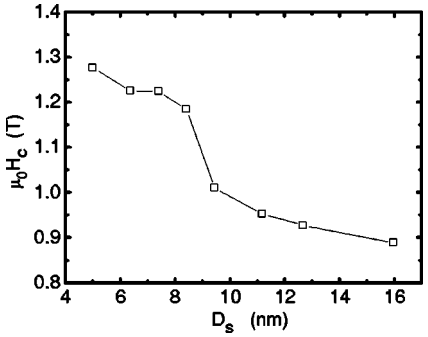


FIG. 4. The dependence of $H_c$ on $D_s$ for the magnets with $D_h=5$ nm and $v_s=15\%$.

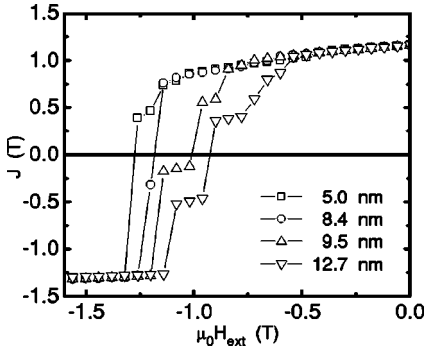


FIG. 5. The typical demagnetization curves for different $D_s$ of the magnets with $D_h=5$ nm and $v_s=15\%$.

can be expressed experimentally as follows:[26]

$$m_r = a - b \ln D, \tag{4}$$

where, the fitting parameters $a$ and $b$ are equal to 0.979 and 0.112, respectively.

The reduction of the coercivity with decreasing $D$ according to Fig. 3(b) can be attributed to the deteriorating effect of the exchange interaction between misoriented grains. Strong misoriented grains are able to induce magnetization reversal of their neighbors (exchange-induced magnetization reversal) and thus the drop of $H_c$.[26] For large $D$, the magnetization reversal of each grain mainly takes place at individual nucleation fields. This simplified model of isolated grains begins to fail as $D$ declines to be smaller than 8–9 nm (about $2\delta_B$) because of the fast increasing $v_{ex}$. However, no simple logarithmic expression[26] between $H_c$ and $D$ is found in Fig. 3(b).

The dependence of $(BH)_{max}$ on $D$ as shown in Fig. 3(c) is found to resemble that of $m_r$ on $D$ since the coercivity obeys the condition $\mu_0 H_c \geqslant J_r/2$. In other words, remanence enhancement is the key to the improvement of $(BH)_{max}$ for the calculated samples. The achieved $(BH)_{max}$ of 34.6 MGOe for $D=3$ nm is larger than the experimental one (about 20.1 MGOe) for $D=5$ nm as reported in Ref. 11. But it is less than 52.8 MGOe for the textured nanocomposite Fe-Pt as in Ref. 8, which reminds us that the alignment of hard grain is important to obtain much higher $(BH)_{max}$.

Figure 4 shows the dependence of $H_c$ on $D_s$ for $D_h=5$ nm and $v_s=15\%$. $H_c$ decreases with increasing $D_s$ particularly fast as $D_s \geqslant 8.4\ \text{nm} \simeq 2\delta_B$. Thus, the critical grain size of soft phase pointed out based on quasi-one-dimensional model[1] is confirmed by the three-dimensional micromagnetic simulation in this work. As $D_s$ is smaller than $2\delta_B$, intergrain exchange interaction can suppress the magnetization reversal of soft magnetic phase and preserve the coercivity in consequence.[1,26,27] Figure 5 gives the demagnetization curves for different $D_s$. It can be found that $m_r$ and $(BH)_{max}$ are nearly unchanged for $D_s$ varying from 5 to 16 nm. This result is similar to the numerical experiments of Ref. 28.

According to the above discussion, $H_c$ keeps a high value when $D_s$ is smaller than $2\delta_B$. However, $H_c$ decreases dramatically with the simultaneous decrease of $D_s$ and $D_h$ (as shown in Fig. 3). Therefore, the grain size of hard phase is also important for high coercivity. The decline of $D_s$ can result in coercivity enhancement only when $D_h$ is properly large.

Traditionally, high remanence and energy product are expected for large $v_s$ because the magnetization of soft phase is usually larger than that of hard phase. Figure 6 shows the calculated $m_r$, $H_c$, and $(BH)_{max}$ as a function of $v_s$ with $D_s=D_h=5$ nm. The numerically calculated magnetic properties are compared with experimental results obtained by H. Zeng *et al.* [11] for the self-assembly nanocomposite $FePt/Fe_3Pt$. It can be found that the dependences of numerical $m_r$ and $H_c$ on $v_s$ are consistent with the experimental results. With increasing $v_s$, $m_r$ increases linearly as $v_s < 15\%$, then decreases as $v_s \geqslant 20\%$. It is impossible for us to guarantee no touched soft grains as $v_s \geqslant 20\%$. Two connected soft grains can be considered as a combined big soft grain. In other words, the soft grain size is enlarged as $v_s \geqslant 20\%$. As a result, the decrease of $m_r$ with increasing $v_s$ can be understood. The monotonous decrease of $H_c$ with increasing $v_s$ is attributed to the low nucleation field of soft phase. High energy products of about 28.1 and 29.1 MGOe are obtained in the samples

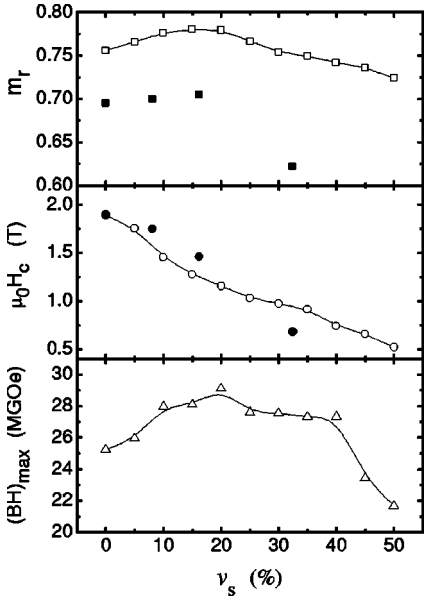


FIG. 6. $m_r$, $H_c$, and $(BH)_{max}$ as functions of $v_s$ for the magnets with $D_s=D_h=5$ nm. The closed symbols refer to the experimental values obtained for $FePt/Fe_3Pt$ self-assembly nanocomposite (see Ref. 11).

with $v_s = 15\%$ and 20%, respectively. Large content of soft phase causes the dramatic decrease of $(BH)_{max}$ because the coercivity no longer obeys the condition of $\mu_0 H_c \geqslant J_r/2$. This result can be confirmed by the small $(BH)_{max}$ of melt-spun $Pr_6Fe_{90}B_4$($Pr_2Fe_{14}B_2$ + 46.1% $\alpha$-Fe) ribbons as reported in Ref. 4. As shown in Fig. 6, there is obvious difference of $m_r$ value between the calculations and the experiments,[11] which results from the different conditions of grain boundaries. The perfect grain boundaries are used in the calculations, whereas transitional region between grains exists in the experiments.[11]

## IV. CONCLUSION

A 3D micromagnetic finite element method was used to investigate the hard magnetic properties of isotropic $FePt/Fe_3Pt$ nanocomposites. The critical grain size of soft phase pointed out based on quasi-one-dimensional model was confirmed by our simulations, i.e., $H_c$ can be improved by decreasing $D_s$ below $2\delta_B$ of hard phase. However, no similar behavior is observed in the dependencies of $m_r$ and $(BH)_{max}$ on $D_s$. The decline of hard grain size $D_h$ leads to the decrease of $H_c$ owing to the exchange-induced magnetization reversal. Properly large $D_h$ is needed for high coercivity in nanocomposites. $(BH)_{max}$ of 34.6 and 28.1 MGOe are achieved for the 3- and 5-nm-scale homogeneous nanocomposite with $v_s = 15\%$, respectively. For high $(BH)_{max}$, the volume fraction of soft phase should not exceed 20%.

## ACKNOWLEDGMENTS

This work was supported by the State Key Project of Fundamental Research and the National Science Foundation of China.

[1] E. F. Kneller and R. Hawig, IEEE Trans. Magn. **27**, 3588 (1991).
[2] R. Skomski, J. Phys.: Condens. Matter **15**, R841 (2003).
[3] A. Manaf, R. A. Buckley, and H. A. Davis, J. Magn. Magn. Mater. **128**, 302 (1993).
[4] D. Goll, M. Seeger, and H. Kronmuller, J. Magn. Magn. Mater. **185**, 49 (1998).
[5] G. C. Hadjipanayis, J. Magn. Magn. Mater. **200**, 373 (1999).
[6] H. W. Zhang, C. B. Rong, J. Zhang, S. Y. Zhang, and B. G. Shen, Phys. Rev. B **66**, 184436 (2002).
[7] J. P. Liu, Y. Liu, and D. J. Sellmyer, J. Appl. Phys. **83**, 6608 (1998).
[8] J. P. Liu, C. P. Luo, Y. Liu, and D. J. Sellmyer, Appl. Phys. Lett. **72**, 483 (1998).
[9] S. Sun, C. B. Murray, D. Weller, L. Folks, and A. Moser, Science **287**, 1989 (2000).
[10] D. J. Sellmyer, Nature (London) **420**, 374 (2002).
[11] H. Zeng, J. Li, J. P. Liu, Z. L. Wang, and S. H. Sun, Nature (London) **420**, 395 (2002).
[12] H. Zeng, S. H. Sun, T. S. Vedantam, J. P. Liu, Z. R. Dai, and Z. L. Wang, Appl. Phys. Lett. **80**, 2583 (2002).
[13] R. Fischer and H. Kronmuller, Phys. Rev. B **54**, 7284 (1996).
[14] J. Fidler and T. Schrefl, J. Phys. D **33**, R135 (2000).
[15] H. W. Zhang, C. B. Rong, X. B. Du, J. Zhang, S. Y. Zhang, and B. G. Shen, Appl. Phys. Lett. **82**, 4098 (2003).
[16] W. F. BrownJr., J. Phys. Soc. Jpn. **17**(Suppl. B-I), 540 (1962).
[17] X. Brunotte, G. Meunier, and J. F. Imhoff, IEEE Trans. Magn. **28**, 1663 (1992).
[18] NAG Fortran library, Mark 20 (Numerical Algorithms Group, Ltd.,Oxford, 2001)
[19] T. Klemmer, D. Hoydick, H. Okumura, B. Zhang, and W. A. Soffa, Scr. Metall. Mater. **33**, 1793 (1995).
[20] S. Okamoto, N. Kikuchi, O. Kitakami, T. Miyazaki, Y. Shimada, and K. Fukamichi, Phys. Rev. B **66**, 024413 (2002).
[21] A. Sakuma, J. Phys. Soc. Jpn. **64**, 4317 (1995).
[22] C. B. Rong, H. W. Zhang, X. B. Du, J. Zhang, S. Y. Zhang, and B. G. Shen, J. Magn. Magn. Mater. (in press).
[23] M. K. Griffiths, J. E. L. Bishop, J. W. Tucker, and H. A. Davies, J. Magn. Magn. Mater. **183**, 49 (1998).
[24] B. Joe, Int. J. Numer. Methods Eng. **37**, 693 (1994).
[25] E. C. Stoner and E. P. Wohlfarth, Philos. Trans. R. Soc. London **240**, 599 (1948).
[26] R. Fischer, T. Schrefl, H. Kronmuller, and J. Fidler, J. Magn. Magn. Mater. **153**, 35 (1996).
[27] M. K. Griffiths, J. E. L. Bishop, J. W. Tucker, and H. A. Davies, J. Magn. Magn. Mater. **234**, 331 (2001).
[28] R. Fischer, T. Leineweber, and H. Kronmuller, Phys. Rev. B **57**, 10723 (1998).